

The PMMA opal film was infiltrated with SiO<sub>2</sub> using a homemade CVD setup operating at atmospheric pressure and room temperature with SiCl<sub>4</sub> and H<sub>2</sub>O as precursors [12]. The CVD process is based on the hydrolysis of silicon tetrachloride (SiCl<sub>4</sub>) on the hydrophilic surface of the spheres; these had been previously wetted with water vapor. SiCl<sub>4</sub> and water are both separately bubbled by a N<sub>2</sub> flow that sweeps the vapor phases to the reactor where the sample is placed. Controlled filling fractions can be achieved by adjusting the N<sub>2</sub>-flow rate and time.

Patterning of the PMMA/SiO<sub>2</sub> composite was performed by EBL, using a Hitachi S-800 and a LEO 1455 scanning electron microscope equipped with a Raith Elphy Plus EBL control unit, at an accelerating voltage of 25 kV and exposure doses between 100 and 850 μC cm<sup>-2</sup>. The samples were developed for 40 s in methyl isobutyl ketone and then placed in isopropanol for 10 s to stop the developing process.

The optical characterization was performed with a FTIR spectrometer, IFS 66 from Bruker with an attached IR Scope II microscope. 15× and 36× Cassegrain objectives were used to focus and collect the light from the patterned motifs. The incident and collected light cover external angles from 5° to 15° (15× objective) and 20° to 57° (36× objective) from normal incidence with respect to the (111) family of planes.

HRSEM was used to observe the alterations in the opal structure. Before examination, samples had been cleaved and sputtered with a thin film of gold.

Received: January 3, 2004  
Final version: May 27, 2004

## Macroscopic Orientation of Block Copolymer Cylinders in Single-Layer Films by Shearing\*\*

By Dan E. Angelescu,\* Judith H. Waller, Douglas H. Adamson, Paru Deshpande, Stephen Y. Chou, Richard A. Register, and Paul M. Chaikin

Block copolymer thin films are currently of great interest as contact masks for inexpensive, large-area lithography. Films of the order of 50 nm thickness, containing a single layer of spherical or cylindrical microdomains formed by one block in a matrix of the other, have been successfully used to pattern semiconductors,<sup>[1–3]</sup> fabricate ultradense arrays of metal<sup>[4,5]</sup> and III–V semiconductor quantum dots,<sup>[6]</sup> and condense and isolate magnetic storage media.<sup>[7,8]</sup> Progress has been impeded by the lack of a versatile technique for inducing long-range order and orientation of the microdomains in a predetermined direction. For example, the striped patterns<sup>[9]</sup> formed by either cylinders or edge-on lamellae—which, if aligned, could serve as precursors to arrays of metal nanowires—instead form curved, wormlike patterns with no long-range order. Techniques capable of aligning these striped patterns over areas of several μm<sup>2</sup> include electric fields,<sup>[10]</sup> graphoepitaxy (where the substrate is topographically prepatterned at the micrometer length scale<sup>[11,12]</sup>), and directional crystallization of a suitable solvent.<sup>[13]</sup> Ordering over even larger areas is potentially achievable by pre patterning the substrate with the desired nanometer-scale pattern,<sup>[14,15]</sup> and then replicating this pattern in the block copolymer film; however, the aim of

- [1] E. Yablonovitch, *Phys. Rev. Lett.* **1987**, *58*, 2085.
- [2] S. John, *Phys. Rev. Lett.* **1987**, *58*, 2486.
- [3] W. M. Lee, S. A. Pruzinsky, P. V. Braun, *Adv. Mater.* **2002**, *14*, 271.
- [4] N. Tétreault, H. Míguez, S. M. Yang, V. Kitaev, G. A. Ozin, *Adv. Mater.* **2003**, *15*, 1167.
- [5] E. Palacios-Lidon, J. F. Galisteo-López, B. H. Juárez, C. López, *Adv. Mater.* **2004**, *16*, 341.
- [6] N. Tétreault, A. Mihi, H. Míguez, I. Rodríguez, G. A. Ozin, F. Mesguier, V. Kitaev, *Adv. Mater.* **2004**, *16*, 346.
- [7] S. G. Romanov, P. Ferrand, M. Egen, R. Zentel, J. Ahopelto, N. Gaponik, A. Eychmüller, A. L. Rogach, C. M. Sotomayor Torres, *Synth. Met.* **2003**, *139*, 701.
- [8] P. Ferrand, M. Egen, R. Zentel, J. Seekamp, S. G. Romanov, C. M. Sotomayor Torres, *Appl. Phys. Lett.* **2003**, *83*, 5289.
- [9] T. Thorsen, S. J. Maerkl, S. R. Quake, *Science* **2002**, *298*, 580.
- [10] W. Tan, T. A. Desai, *Biomaterials* **2004**, *25*, 1355.
- [11] P. Jiang, J. F. Bertone, K. S. Hwang, V. L. Colvin, *Chem. Mater.* **1999**, *11*, 2132.
- [12] H. Míguez, N. Tétreault, B. Hatton, S. M. Yang, D. Perovic, G. A. Ozin, *Chem. Commun.* **2002**, *14*, 2736.
- [13] S. G. Johnson, J. D. Joannopoulos, *Optics Exp.* **2001**, *8*, 173.
- [14] J. F. Galisteo-López, E. Palacios-Lidon, E. Castillo-Martinez, C. López, *Phys. Rev. B* **2003**, *68*, 115109.
- [15] M. Müller, R. Zentel, T. Maka, S. G. Romanov, C. M. Sotomayor Torres, *Chem. Mater.* **2000**, *12*, 2508.

- [\*] Dr. D. E. Angelescu<sup>[+]</sup>  
Department of Physics, Princeton University  
Princeton, NJ 08544 (USA)  
E-mail: angelscu@alumni.princeton.edu
- J. H. Waller  
Department of Materials Science  
Oxford University, Oxford (UK)
- Dr. D. H. Adamson  
Princeton Materials Institute, Princeton University  
Princeton, NJ 08544 (USA)
- P. Deshpande, Prof. S. Y. Chou  
Department of Electrical Engineering, Princeton University  
Princeton, NJ 08544 (USA)
- Prof. R. A. Register  
Department of Chemical Engineering, Princeton University  
Princeton, NJ 08544 (USA)
- Prof. P. M. Chaikin  
Department of Physics, Princeton University  
Princeton, NJ 08544 (USA)

[+] Present address: Schlumberger-Doll Research, 36 Old Quarry Rd., Ridgefield CT 06877, USA.

[\*\*] We gratefully acknowledge financial support from the National Science Foundation through the Princeton Center for Complex Materials (DMR-0213706). This work utilized processes and device designs developed at the NIST Combinatorial Methods Center in Gaithersburg, MD.

lithography is to impart the pattern to featureless substrates, preferably of any composition.

Shear is a well-established means of aligning block copolymers in bulk; cylinder-forming block copolymers respond by orienting cylinder axes parallel to the flow direction, and macroscopic specimens with near-single-crystal texture can be obtained.<sup>[16,17]</sup> Flow of block copolymer solutions on inclined substrates can also produce alignment in relatively thick films, containing approximately ten layers of cylinders.<sup>[18]</sup> However, neither flow nor shearing has been previously employed on the single-layer films desired for lithography, perhaps because of the apparent difficulty in imparting uniform shear to a film only 50 nm thick. Here we present a method for achieving this aim, by subjecting these ultrathin block copolymer films to unidirectional shear. Our new shearing technique provides a simple, scalable pathway to single-layer copolymer alignment, which is ideally suited for quantitative investigations and does not use any specialized laboratory equipment.

A monolayer film of diblock copolymer was applied on a polished Si substrate and placed on a hotplate; an unpatterned elastomer pad was then pressed onto the film using a weight. A controlled lateral force was applied to the weight and its displacement monitored, while the Si substrate was restricted from moving; this experimental setup is schematically represented in the inset to Figure 1. The resulting shear stress (typically  $\sigma \approx 10^4$  Pa) caused the immediate elastic distortion of the poly(dimethylsiloxane) (PDMS) pad and was followed by slow linear displacement, indicating viscous shear flow of the copolymer film (Fig. 1). Typically, the shear stress was applied

for an hour, leading to  $\approx 1$  mm measured displacements of the PDMS pad. Translation velocity after the application of shear stress was measured to be  $\approx 300$  nm s<sup>-1</sup> (shear rate 10 s<sup>-1</sup>), which allows calculation of an apparent thin-film viscosity  $\sigma \approx 10^3$  Pa s (this value ignores possible slip at the interfaces of the polymer layer). This result is consistent with bulk rheological measurements on sphere-forming polystyrene–poly(ethylene-*alt*-propylene) (PS–PEP) systems of similar total molecular weight past a characteristic yield stress  $\sigma_0 \approx 360$  Pa, above which X-ray diffraction studies reveal a disordered structure.<sup>[19]</sup> Despite the fact that we use a cylinder-forming rather than a sphere-forming PS–PEP system, the high shear stresses used ( $\sigma \approx 28 \sigma_0$ ) should also be capable of disordering (and destroying) the cylindrical microdomains which are misaligned.

Atomic force microscopy (AFM) images of a PS–PEP copolymer sample after annealing at 100 °C under shear are shown in Figures 2a,b. The micrographs, acquired 8 mm apart from one another, are characteristic for the degree of alignment existing in the sample. No disclinations are present and the orientational correlation length of the pattern is essentially infinite. The only imperfections are caused by slight meandering of the cylinders about the shearing direction and by the existence of dislocations, although at a lower (by one order of magnitude) density than in samples annealed under the same conditions but without shearing. Nonsheared samples display characteristic fingerprint-like patterns,<sup>[20]</sup> where disclinations limit the correlation length to  $\approx 300$  nm (Fig. 2c).

We investigated the dependence of alignment quality, as quantified by the density of dislocations (Fig. 3a) and the root mean square (RMS) spread,  $\langle(\Delta\theta)^2\rangle^{1/2}$ , of the alignment angle (Fig. 3b), on the thickness of the polymer film. To this end, a film incorporating a thickness gradient was sheared perpendicular to the direction of the gradient. The results imply that alignment quality is best when the film thickness is within a 2 nm window centered around the monolayer thickness, which corresponds to 30 nm for this particular polymer system. Both the density of dislocations and the RMS angular spread increase rather rapidly for thicknesses smaller than a monolayer, and also increase, although less dramatically, for larger thicknesses. We have also investigated the effects of varying the shear rate on alignment quality. There is no apparent dependence on the shear rate over the 40 nm s<sup>-1</sup> to 500 nm s<sup>-1</sup> range. Shear rates below 40 nm s<sup>-1</sup> could not be reliably produced due to competing uncontrolled shear caused by the thermal expansion of the PDMS pad. Some other factors can affect the alignment: very short annealing times (a few minutes) produce alignment, but of significantly lower quality; the alignment quality is also degraded in close proximity (200  $\mu$ m) to the PDMS pad edge.

As previously reported, the large shear stress values we used place our experiments far into the regime where microdomains can be disordered and

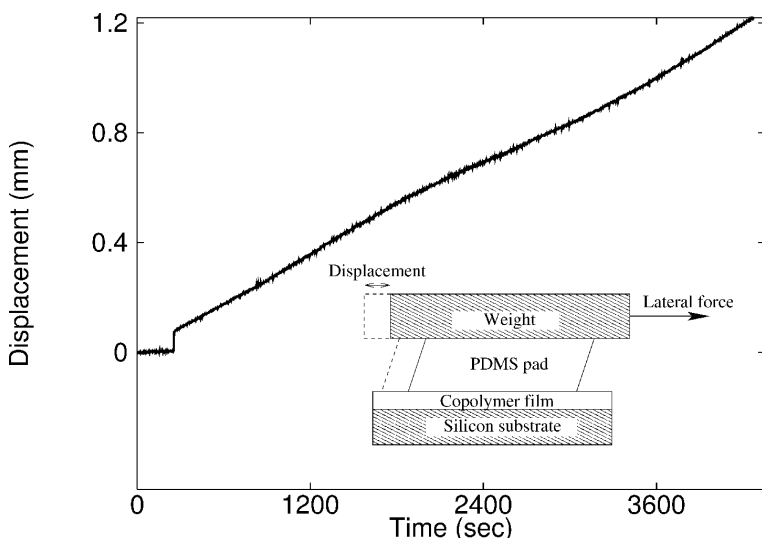


**Figure 1.** Shearing experiment: displacement data from the optical position sensor. A PDMS pad is subjected to a lateral force at  $t \approx 300$  s causing an immediate elastic deformation of the pad, followed by the displacement of the PDMS pad at constant speed. The inset shows a schematic diagram of the setup: the 1 cm<sup>2</sup> PDMS pad is pressed with a  $\approx 1$  kg weight against the polymer film on a heated silicon substrate, and a  $\approx 1$  N lateral force is applied (schematic not to scale: typical copolymer film thickness 30 nm, typical PDMS pad thickness 1 mm). The resulting displacement is monitored with a laser–mirror–optical sensor setup (not shown).

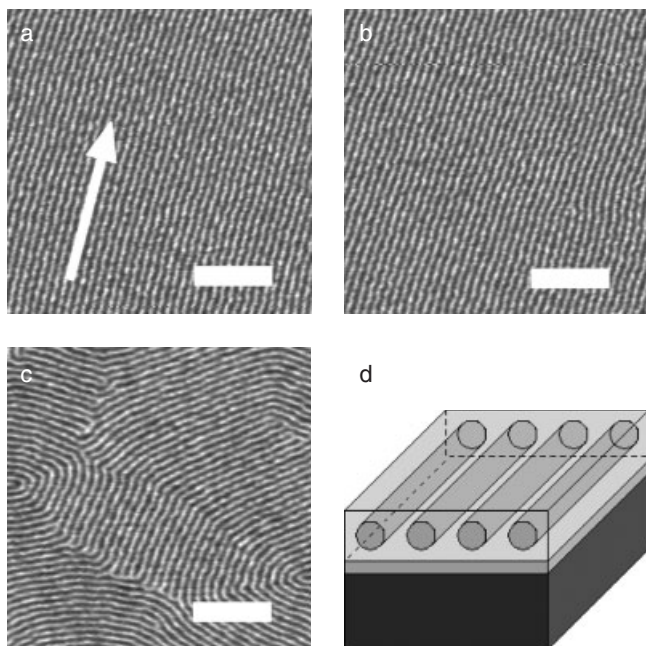


**Figure 2.** a) An AFM micrograph acquired on a copolymer sample aligned by the method described in this paper. The cylindrical microdomains are in perfect registry, without any visible defect. The arrow indicates the shearing direction. b) Another micrograph, acquired 8 mm away from the one shown in (a). A single dislocation is visible (these are particularly well-aligned regions) c) Fingerprint-like pattern characteristic of samples annealed without shearing. Scale bar = 250 nm. d) Cartoon of a single layer of cylindrical microdomains. PS cylinders (darker gray) form within a matrix of PEP (lighter gray), with a PS wetting layer at the Si interface. Film thickness: 30 nm.

destroyed by shear. Shearing can induce both ordering (at low shear rates) and disordering (at higher rates) in concentrated solutions of cylinder-forming diblocks.<sup>[21]</sup> A suggestion was made by the authors of that study that shear rates higher than the inverse relaxation time,  $\tau_r$ , of cylinder fluctuations could lead to disordering, the cylinders not being able to react fast enough to the imposed shear.

The shear disordering time depends, in the case of cylindrical microdomains, on the orientation angle,  $\theta$ , of the cylinder normal with respect to the shear. Cylinders parallel to the shear direction will not be affected by shear ( $\tau_d(\theta = \pi/2) = \infty$ ). Cylinders perpendicular to the shear will be destroyed as soon as the strain becomes of the order of 1 (i.e., an inter-cylinder spacing); the corresponding time is  $\tau_d(\theta = 0) = 1/\dot{\gamma}$ , where by  $\dot{\gamma}$  we denote the shear rate. For an intermediate orientation,  $\tau_d(\theta) = 1/(|\cos(\theta)| \dot{\gamma})$ , or  $\tau_r/\tau_d = \tau_r |\cos(\theta)| \dot{\gamma}$ .

The two-dimensional dynamics of microphase separation have been previously modeled and simulated using a modified Cahn–Hilliard equation<sup>[22,23]</sup> with a cell dynamics treatment.<sup>[23,24]</sup> In the presence of shear the anisotropic destruction of the periodically ordered cylinders changes the rate of their formation, which can be incorporated into the modified Cahn–Hilliard equation via a term of the form  $(|\cos(\theta)| \dot{\gamma})^2$  (squared due to analyticity and symmetry requirements). This is conveniently incorporated as  $(\dot{\gamma} \nabla)^2$  or, for shear along  $x$ , as

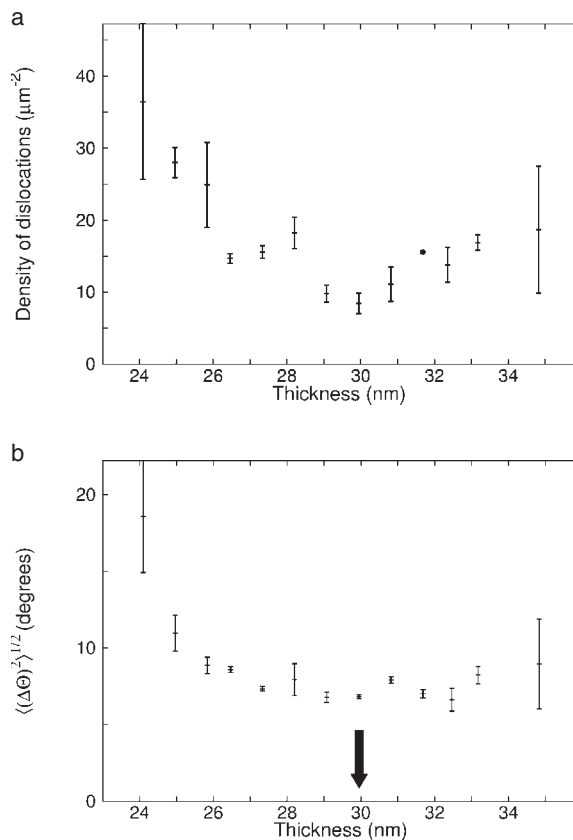


**Figure 3.** The alignment quality (as quantified by the dislocation density (a) and by the RMS angular spread (b) of the pattern) depends on the thickness of the film. The best alignment is obtained for thicknesses close to that of a single layer (indicated by arrow in (b)). The error bars were obtained by collecting data from three independent micrographs for each thickness.

$(D_x/2)(\partial_x)^2$ , an effective anisotropic diffusion term with coefficient  $D_x = a(\dot{\gamma} \tau_r)^2$ ,  $a$  being a phenomenological constant of order unity. Intuitively, the two-dimensional simulation can be regarded as a plane projection of the sheared monolayer, with the enhanced diffusion term arising from the smearing in the  $x$  direction introduced by shearing. Since, in modified Cahn–Hilliard,  $T_{ODT}$  (bulk order–disorder-transition temperature) also appears in a quadratic term in the order parameter, the new shear term can be interpreted as an effective anisotropic reduction in the bulk order–disorder-transition temperature,  $T_{ODT}$ ,  $T_{ODT} \rightarrow T_{ODT} - a'(k\tau_r |\cos(\theta)| \dot{\gamma})^2$  with  $a'$  being a phenomenological constant and  $k$  the reciprocal wavevector corresponding to the periodic spatial variation.

In order to test our model, we have performed numerical simulations<sup>[23]</sup> with the shear terms included (details elsewhere<sup>[25]</sup>). The results are summarized in Figure 4. Shear, introduced as explained above through an anisotropic diffusion term, is seen to generate alignment of the microdomains with the shear direction. At very low shear rates, the alignment quality is seen to degrade (and, as expected, the pattern becomes completely isotropic in the zero shearing limit). We point out that the results presented here involve different

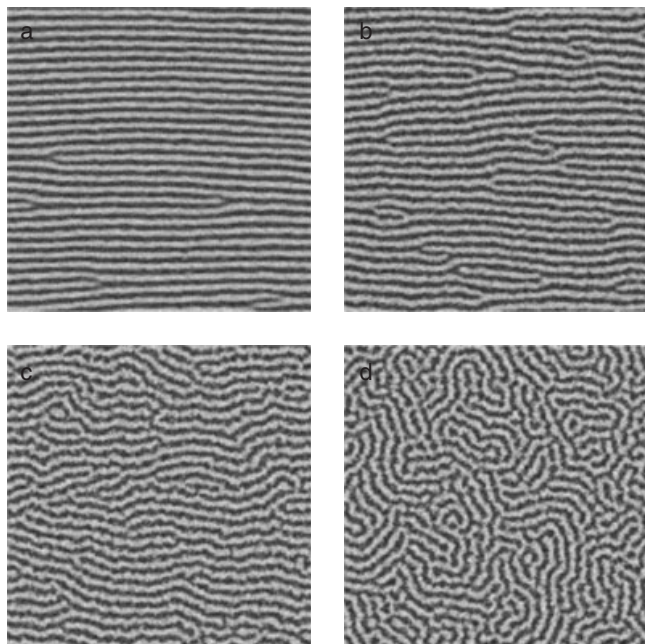


**Figure 4.** Cell dynamics simulations demonstrating long-range alignment via shear; decreasing  $D_x = a(\dot{\gamma} \tau_r)^2$  (or, equivalently, decreasing the shear rate  $\dot{\gamma}$ ) leads to a visible degradation of the alignment quality. a)  $D_x = 0.40$ ; b)  $D_x = 0.10$ ; c)  $D_x = 0.01$ ; d)  $D_x = 0$  (portions of larger simulations shown).

physics from previous numerical studies of shear alignment in diblock copolymers, underscoring the differences in shear alignment of thin films versus bulk. Previous simulations<sup>[23,26]</sup> focused either on shear in bulk lamellar samples, or on shear with the vorticity direction out of the sample plane. Our work involves sheared thin films, where the vorticity would be in the plane of the film (since our simulation is essentially two-dimensional, vorticity is not properly defined).

It is important to note that in this simple model, films of block copolymers which form spherical microdomains would not show alignment. This is consistent with our findings, from both experiments and simulations.<sup>[25]</sup> An order of magnitude estimate is necessary in order to check the applicability of this model to our copolymer system. We typically use shear rates of  $\dot{\gamma} = 10 \text{ s}^{-1}$ . The fluctuation relaxation time  $\tau_r$  can be estimated as the time it takes a molecule to diffuse a distance equal to a lattice spacing  $\lambda = 25 \text{ nm}$ . We therefore have  $\tau_r = \lambda^2/D_0$ , where  $D_0$  is the polymer diffusion coefficient.  $D_0$  has been measured for several diblock copolymer systems similar to ours,<sup>[27–29]</sup> the values lie in the  $10^{-17}$  to  $10^{-15} \text{ m}^2 \text{ s}^{-1}$  range, leading to  $\dot{\gamma} \tau_r$  of 0.6 to 60. The model should therefore be applicable to our copolymer system. The shear rate below which the pattern quality visibly degrades, however, may be very small.

Our technique is easily modified for larger or smaller areas (by changing the size of the elastomer pad) as well as for other geometries (e.g. patterns consisting of concentric circles). Since stress and strain are monitored during the process, this technique should also prove a useful tool for fundamental

studies of linear and nonlinear viscosity and elasticity, and shear melting and alignment in a well controlled and constrained geometry.

## Experimental

We used a polystyrene–poly(ethylene-*alt*-propylene) (PS–PEP) diblock copolymer (molecular weights PS:  $4.9 \text{ kg mol}^{-1}$ ; PEP:  $13.2 \text{ kg mol}^{-1}$ ) that was synthesized by means of living anionic polymerization and hydrogenation following standard procedures [19]. The polymer exhibited an upper glass-transition temperature  $T_g \approx 60 \text{ }^\circ\text{C}$  corresponding to the PS block, and a bulk order–disorder-transition temperature  $T_{\text{ODT}} = 144 \pm 2 \text{ }^\circ\text{C}$ , as measured by small angle X-ray scattering. The bulk copolymer morphology consisted of cylindrical PS microdomains embedded in a PEP matrix. Monolayer (30 nm thickness) films on polished Si substrates were prepared by spin-coating from a dilute (1%) toluene solution. This method of preparation resulted in highly uniform film thickness; samples incorporating a thickness gradient (obtained by a flow-coating technique [30]) were also employed. The through-film morphology of the polymer monolayer, revealed by means of dynamical secondary ion mass spectroscopy [25], involved a PS wetting layer at the Si interface; the air (and presumably PDMS) interface was wet by PEP, leading to the thin-film morphology schematically shown in Figure 2d.

The  $1 \text{ cm} \times 1 \text{ cm} \times 0.1 \text{ cm}$  elastomer pad was prepared from polydimethylsiloxane (PDMS, Dow Corning Sylgard 184), and cured (1 h at  $60 \text{ }^\circ\text{C}$ ) between a polished Si wafer and a glass slide. Spacers were used to control the thickness of the pad.

The fabricated pad was pressed onto the PS–PEP monolayer using a 1 kg weight. The annealing temperature was controlled using a precision hotplate. Typically, the experiment was started with the hotplate cold and no horizontal force applied. The temperature was then ramped up to a value (typically  $100 \text{ }^\circ\text{C}$ ) between  $T_g$  and  $T_{\text{ODT}}$ , and a horizontal force (typically 1 N) was subsequently applied using a weight-over-pulley arrangement (Fig. 1, inset), resulting in a  $\sigma \approx 10^4 \text{ Pa}$  shear stress throughout the copolymer film. The displacement of the pad was monitored by a laser–mirror–detector assembly, with the mirror attached to the 1 kg weight.

Received: April 29, 2004

Final version: August 1, 2004

Published online: September 16, 2004

- [1] M. Park, C. Harrison, P. M. Chaikin, R. A. Register, D. H. Adamson, *Science* **1997**, 276, 1401.
- [2] H. C. Kim, X. Q. Jia, C. M. Stafford, D. H. Kim, T. J. McCarthy, M. Tuominen, C. J. Hawker, T. P. Russell, *Adv. Mater.* **2001**, 13, 795.
- [3] K. W. Guarini, C. T. Black, Y. Zhang, H. Kim, E. M. Sikorski, I. V. Babich, *J. Vac. Sci. Technol. B* **2002**, 20, 2788.
- [4] M. Park, P. M. Chaikin, R. A. Register, D. H. Adamson, *Appl. Phys. Lett.* **2001**, 79, 257.
- [5] K. Shin, K. A. Leach, J. T. Goldbach, D. H. Kim, J. Y. Jho, M. Tuominen, C. J. Hawker, T. P. Russell, *Nano Lett.* **2002**, 2, 933.
- [6] R. R. Li, P. D. Dapkus, M. E. Thompson, W. G. Jeong, C. K. Harrison, P. M. Chaikin, R. A. Register, D. H. Adamson, *Appl. Phys. Lett.* **2000**, 76, 1689.
- [7] J. Y. Cheng, C. A. Ross, V. Z. H. Chan, E. L. Thomas, R. G. H. Lammertink, G. J. Vancso, *Adv. Mater.* **2001**, 13, 1174.
- [8] K. Naito, H. Hieda, M. Sakurai, Y. Kamata, K. Asakawa, *IEEE Trans. Magn.* **2002**, 38, 1949.
- [9] C. Harrison, D. H. Adamson, Z. Cheng, J. M. Sebastian, S. Sethuraman, D. A. Huse, R. A. Register, P. M. Chaikin, *Science* **2000**, 290, 1558.
- [10] T. L. Morkved, M. Lu, A. M. Urbas, E. E. Ehrichs, H. M. Jaeger, P. Mansky, T. P. Russell, *Science* **1996**, 273, 931.

- [11] R. A. Segalman, H. Yokoyama, E. J. Kramer, *Adv. Mater.* **2001**, *13*, 1152.
- [12] M. Trawick, D. Angelescu, P. Chaikin, J. Sebastian, R. Register, D. Adamson, C. Harrison, *Bull. Am. Phys. Soc.* **2002**, *47*, 970.
- [13] C. Park, C. De Rosa, E. L. Thomas, *Macromolecules* **2001**, *34*, 2602.
- [14] L. Rockford, Y. Liu, P. Mansky, T. P. Russell, M. Yoon, S. G. J. Mochrie, *Phys. Rev. Lett.* **1999**, *82*, 2602.
- [15] S. O. Kim, H. H. Solak, M. P. Stoykovich, N. J. Ferrier, J. J. de Pablo, P. F. Nealey, *Nature* **2003**, *424*, 411.
- [16] A. Keller, E. Pedemonte, F. M. Willmouth, *Nature* **1970**, *225*, 538.
- [17] G. Hadziioannou, A. Mathis, A. Skoulios, *Colloid Polym. Sci.* **1979**, *257*, 136.
- [18] M. Kimura, M. J. Misner, T. Xu, S. H. Kim, and T. P. Russell, *Langmuir* **2003**, *19*, 9910.
- [19] J. M. Sebastian, C. Lai, W. W. Graessley, R. A. Register, *Macromolecules* **2002**, *35*, 2707.
- [20] C. Harrison, Z. Cheng, S. Sethuraman, D. Huse, P. M. Chaikin, D. A. Vega, J. M. Sebastian, R. A. Register, D. H. Adamson, *Phys. Rev. E* **2002**, *66*, 011706.
- [21] N. P. Balsara, H. J. Dai, *J. Chem. Phys.* **1996**, *105*, 2942.
- [22] P. M. Chaikin, T. C. Lubensky, *Principles of Condensed Matter Physics*, Cambridge University Press, Cambridge, UK **1995**.
- [23] I. W. Hamley, *Macromol. Theory Simul.* **2000**, *9*, 363.
- [24] M. Bahiana, Y. Oono, *Phys. Rev. A* **1990**, *41*, 6763.
- [25] D. E. Angelescu, *Ph. D. Thesis*, Princeton University, **2003**.
- [26] S. R. Ren, I. W. Hamley, *Phys. Rev. E* **2001**, *63*, 041503.
- [27] M. W. Hamersky, M. Tirrell, T. P. Lodge, *Langmuir* **1998**, *14*, 6974.
- [28] M. C. Dalvi, C. E. Eastman, T. P. Lodge, *Phys. Rev. Lett.* **1993**, *71*, 2591.
- [29] C. E. Eastman, T. P. Lodge, *Macromolecules* **1993**, *27*, 5591.
- [30] J. C. Meredith, A. P. Smith, A. Karim, E. J. Amis, *Macromolecules* **2000**, *33*, 9747.

## Self-Catalysis and Phase Transformation in the Formation of CdSe Nanosaws\*\*

By Yong Ding, Christopher Ma, and Zhong Lin Wang\*

Wurtzite-structured CdSe is an important type II–V semiconducting compound for optoelectronics.<sup>[1,2]</sup> Due to the high precision of size controllability, CdSe quantum dots are the most extensively studied quantum nanostructure, and they have been used as a model system for investigating a wide range of nanoscale electronic, optical, optoelectronic, and chemical processes.<sup>[3,4]</sup> Although studies of CdSe have been carried out for more than a dozen years, there are only a few reports on the synthesis of quasi-one-dimensional CdSe nano-

structures. Shape-controlled synthesis of CdSe nanorods,<sup>[5,6]</sup> and template-assisted synthesis of CdSe nanowires<sup>[7]</sup> and nanotubes<sup>[8]</sup> have been demonstrated using electrochemical and chemical approaches. Two-dimensional arrays of CdSe pillars have been fabricated using electron-beam lithography.<sup>[9]</sup> These nanowires and nanotubes are composed of nanometer-sized grains, and are polycrystalline in nature. Recently, we reported a single-crystal nanobelt/nanoribbon structure of wurtzite CdSe, parts of which display a “saw” shape.<sup>[10]</sup>

In this communication, a detailed structural analysis of the formation process of CdSe nanosheets and nanosaws is presented. The CdSe nanostructures have an identical growth direction of  $[01\bar{1}0]$ , and top and bottom surface planes of  $(2\bar{1}10)$  across a large temperature zone. The growth of the special tooth-shaped saw structure is suggested to be a combined result of secondary epitaxial-nucleation processes owing to zinc-blende–wurtzite phase transformations and to the self-catalytic effect of the Cd-terminated  $(0001)$  surface.<sup>[11,12]</sup>

The CdSe nanobelts were synthesized by a thermal-evaporation process in a horizontal-tube furnace.<sup>[10]</sup> The as-synthesized samples were first analyzed by scanning electron microscopy (SEM) to find the relationship between the deposition temperature and their growth morphologies. The SEM images of the samples collected in low-temperature ( $\sim 600^\circ\text{C}$ ) and high-temperature ( $\sim 700^\circ\text{C}$ ) regions are shown in Figures 1a,b, respectively. The plot in Figure 1c depicts the relationship between the local substrate temperature and the distance from the center of the furnace. The length of the silicon substrate used in our experiment is around 10 cm and its position in the furnace is illustrated in Figure 1c. The SEM images in Figures 1a,b were obtained from the regions marked a and b in Figure 1c, corresponding to temperatures of  $\sim 600$  and  $\sim 700^\circ\text{C}$ , respectively. The SEM images reveal that the samples in the lower and higher temperature regions show nanobelt/nanosheet and nanosaw structures, respectively.

The structures of the nanobelts/nanosheets and nanosaws have been analyzed to understand the temperature dependence of the growth morphology. Figure 2a is a low-magnification transmission electron microscopy (TEM) image of a nanobelt/nanosheet collected in the lower-temperature region. The length and width are hundreds and several micrometers, respectively, while the thickness of the nanobelt is no more than 20 nm, as indicated by the bending area of the belt, which has a typical sheet morphology. The selected area electron diffraction (SAED) pattern (Fig. 2a, inset) indicates that the nanobelt/nanosheet has a wurtzite structure, and grows along  $[01\bar{1}0]$ . After examining more than fifty belts from the same temperature region, only one of them grows along  $[0001]$ , while the remaining ones grow along  $[01\bar{1}0]$ . High-resolution TEM (HRTEM) imaging confirms the growth direction of the belt (Fig. 2b). Despite the uniform thickness of the belt, the surfaces on either side are not parallel to each other. The surface on one side is the perfect  $(0001)$  plane, but the surface on the other side has steps, indicating asymmetric surface activities on the Cd-terminated  $(0001)$  and Se-terminated  $(000\bar{1})$  surfaces, analogous to the case of ZnO.<sup>[11]</sup>

[\*] Prof. Z. L. Wang, Dr. Y. Ding, C. Ma  
School of Materials Science and Engineering  
Georgia Institute of Technology  
Atlanta, GA 30332-0245 (USA)  
E-mail: zhong.wang@mse.gatech.edu

[\*\*] Thanks to the financial support from the US NSF NIRT ECS-0210332. Thanks to Daniel Moore for calibrating the furnace.